ELSEVIER

Journal of Immunological Methods 236 (2000) 147–165

JOURNAL OF IMMUNOLOGICAL METHODS

www.elsevier.nl/locate/jim

Recombinant Technology

Characterizing the functionality of recombinant T-cell receptors in vitro: a pMHC tetramer based approach

Alain C. Tissot, Frédéric Pecorari, Andreas Plückthun*

Biochemisches Institut, Universität Zürich, Winterthurstrasse 190, CH-8057 Zürich, Switzerland

Received 30 July 1999; accepted 12 November 1999

Abstract

The very low affinity of the T-cell receptor (TCR) for the peptide-major histocompatibility complex (pMHC) has made it very challenging to design assays for testing the functionality of these molecules on small scales, which in turn has severely hampered the progress in developing expression and refolding methodologies for the TCR. We have now developed an ELISA assay for detecting pMHC binding to functional recombinant TCRs. It uses tetramers of biotinylated pMHCs bound to a neutravidin–horseradish peroxidase conjugate and detects the presence of functional TCR, bound in a productive orientation to an immobilized anti-Cβ antibody. Specificity can be stringently demonstrated by inhibition with monomeric pMHCs. The assay is very sensitive and specific, and requires only very small amounts of protein. It has allowed us to study the unstable recombinant TCR P14, which we expressed and refolded from *Escherichia coli*. The TCR P14 is directed against the most abundant epitope of LCMV. We have confirmed the specificity of the interaction by BIAcore, and were able to determine the dissociation constant of the interaction of the P14 TCR and of the gp33-pMHC as 6 μM. This affinity ranks it among the tighter ones of TCR–pMHC interactions, and unusually low affinity thus does not seem to be the cause of the modest protective power of these T-cells, compared to others elicited in the anti-LCMV response. This strategy of multimerizing one partner and immobilizing the other in both a native form and productive orientation should be generally useful for characterizing the weak interactions of cell-surface molecules.

Keywords: TCR; MHC-tetramer; Protein folding; Receptor–ligand interactions; Binding assay

Abbreviations: APC, antigen presenting cell; BSA, bovine serum albumin; CDR, complementarity determining region; CTL, cytotoxic T-lymphocyte; DTT, dithiothreitol; EDC, *N*-(3-dimethylaminopropyl)-*N′*-ethyl-carbodiimide-hydrochloride; ELISA, enzyme-linked immunosorbent assay; flu, influenza nucleoprotein epitope np366–374; HBS, HEPES-buffered saline; HRP, horseradish peroxidase; IPTG, isopropyl-β-D-1-thiogalactopyranoside; Gdn–HCl, guanidine hydrochloride; LCMV, lymphocytic choriomeningitis virus; MHC, major histocompatibility complex; Nav–HRP, neutravidin–horseradish peroxidase conjugate; NHS, N-hydroxysuccinimide; PAGE, polyacrylamide gel electrophoresis; pMHC, complex of peptide and MHC; RT, room temperature; SDS, sodiumdodecyl sulfate; SPR, surface plasmon resonance; TBS, Tris-buffered saline; TCR, T-cell receptor

*Corresponding author. Fax: +41-1-635-5712.

E-mail address: plueckthun@biocfebs.unizh.ch (A. Plückthun)

0022-1759/00/$ – see front matter
PII: S0022-1759(99)00226-4

1. Introduction

The crucial decision of the immune system, self or non-self, with all of its consequence in health and disease, is based on a quantitative read-out of binding energies between the peptide-major histocompatibility complex (pMHC) and the T-cell receptor (TCR). To understand this at the molecular level, with the vision of being able to manipulate it, it is essential to have facile access to quantitative data, both binding affinity and kinetics, and to 3D-structural data of the complex. While affinity data (reviewed in Davis et al., 1998) and crystallographic data (Garboczi et al., 1996a; Garcia et al., 1996; Ding et al., 1998; Garcia et al., 1998; Wang et al., 1998) have been reported for a few pMHC–TCR systems, many more structures will be necessary to reach an understanding of the structure–activity relationship at the required level of detail.

The stumbling block has been the preparation of TCR in sufficient amounts and in good quality, i.e. with the native structure. Again, several examples using a variety of expression systems have been reported (Lin et al., 1990; Weber et al., 1992; Chang et al., 1994; Chung et al., 1994; Wülfing and Plückthun, 1994; Alam et al., 1996; Garboczi et al., 1996b; Golden et al., 1997; Khandekar et al., 1997; Plaksin et al., 1997; Pecorari et al., 1999). The problem for all of this work, however, has been to quantitatively assess the proper folding of the TCR, and to quantitatively characterize its binding to the pMHC complex.

The central problem is that the affinity of the pMHC–TCR interaction is very weak. To detect this interaction, high concentrations of the components are therefore necessary, which is very inconvenient for the development of expression systems, refolding methodologies or any quantitative or routine assay. Furthermore, all assays have to take into account the potential intrinsic instability of the TCR, and allow its immobilization in the native state. We have now solved these problems by using tetrameric pMHC in conjunction with refolded and productively immobilized TCR in a general way.

Only few methods are available to measure interactions with K_D values of 10^{-4}–10^{-6} M. While surface plasmon resonance (SPR) and native PAGE have been described (Corr et al., 1994; Garboczi et al., 1996b), they require purified components and are not suitable for even medium throughput assays. Native PAGE has the additional disadvantage of involving the separation of the complexed and free forms of the proteins, which can lead to dissociation of complexes during migration. Indeed, it failed to show complexes with K_D values of 10^{-4} M (Pecorari et al., unpublished). The BIAcore method is one of the few methods available for studying weak interactions, but these weak interactions requires very high concentrations of protein. This can often be the bottleneck when dealing with unstable molecules, and prevent their characterization. Furthermore, it cannot be carried out with impure fractions during the purification procedure.

There are several examples where nature uses multimeric interactions to confer high functional affinity (avidity) to intrinsically weak monomeric interactions (van der Merwe and Barclay, 1994; Chothia and Jones, 1997), and this strategy has also been used to engineer mini-antibodies for high avidity (Pack and Plückthun, 1992; Plückthun and Pack, 1997). Multimerization of weak binding domains (Dal Porto et al., 1993) has the advantage of increasing binding and specificity at the same time (Klemm et al., 1998). This avidity effect is well documented in the case of cell adhesion molecules (Chothia and Jones, 1997).

The recently developed pMHC tetramer staining method of Altman et al. (1996) makes use of this effect by tetramerizing in vitro biotinylated pMHCs on streptavidin, conjugated to phycoerythrin. These reagents have already found widespread applications (Dunbar et al., 1998; McMichael and O'Callaghan, 1998; Murali-Krishna et al., 1998; Gallimore et al., 1998b) and have given for the first time a general method of identifying T-cell clones through the molecule which they recognize, the pMHC.

We have adapted this method to use it with recombinant proteins outside the context of the cell, in the convenient format of an ELISA assay. This has allowed us for the first time to have an assay on a microscale which functionally assesses the weak affinity between pMHC and TCR, using recombinant, in vitro refolded molecules. Thus, we now have a methodology at hand for not only testing the functionality of proteins expressed and refolded from *E. coli*, but one which is in principle extendible to all

other expression hosts producing soluble TCRs. Provided that a protein can be biotinylated at one of its termini, this assay can be useful for any low affinity ligand–receptor interaction.

We applied our assay to the optimization of the expression, refolding and characterization of the P14 TCR. The P14 TCR is derived from the cytotoxic T-lymphocyte (CTL) clone P14, and is specific for the epitope gp33 of the LCMV viral glycoprotein, presented by the class I MHC H-2D^b (Pircher et al., 1987; Pircher et al., 1993). We have used as controls the other major H-2D^b restricted epitopes of the immune answer to LCMV, the peptide gp276 of the same viral glycoprotein, and np396 of the nucleoprotein (Hudrisier et al., 1996; Gallimore et al., 1998a). We also used two other unrelated H-2D^b restricted epitopes as controls, the myhsp60 peptide, derived from the *Mycobacterium bovis* Hsp60 (Schoel et al., 1994; Pecorari et al., 1999), and an epitope of the influenza nucleoprotein, np366–374 of the influenza virus nucleoprotein (Townsend et al., 1986; Young et al., 1994).

During the immune response to the virus strain LCMV-WE, much of the cytotoxic T-cell response is directed against the epitope gp33, but this does not seem to correlate with the protective power of the CTLs (Gallimore et al., 1998a). Since the epitope density of the naturally processed peptides of LCMV, as well as the relative density of TCRs on the CTLs are now known (Gallimore et al., 1998a), it was interesting to characterize the affinity of the P14 TCR to see whether the postulated lower activity for the CTLs of the gp33 specificity could be attributed to a low affinity TCR. We show here that this is not the case. The protective power must thus depend on other factors.

2. Materials and methods

2.1. Materials

The peptides were synthesized by Chiron Technologies (Clayton Victoria, Australia) to 95% purity and checked by mass spectrometry analysis. The peptides had the following sequences: myhsp60 peptide: SALQNAASIA, gp33–41 (gp33): KAVYNFATM, gp276–286 (gp276): SGVENPGGYCL, np396–404 (np396): FQPQNGQFI, flu: ASNENMETM. The flu peptide corresponds to the epitope np366–374 of the influenza virus nucleoprotein (Townsend et al., 1986).

Tris-buffered saline (TBS) buffer is 20 mM Tris–HCl, 150 mM NaCl, pH 8.0. HEPES-buffered saline (HBS) buffer is 20 mM HEPES, 150 mM NaCl, pH 7.4. N-hydroxysuccinimide (NHS) and *N*-(3-dimethylaminopropyl)-*N′*-ethyl-carbodiimide-hydrochloride (EDC) were from Fluka (Buchs, Switzerland).

The plasmids encoding H-2D^b and β_2-microglobulin (Young et al., 1994) were obtained from Dr. J. C. Sacchettini (Department of Biochemistry, Albert Einstein College of Medicine, New York, USA).

2.2. Construction of expression plasmids

The genes of the α- and β-chain of the P14 TCR were amplified by PCR from the cDNA clones of Pircher et al. (1987). The N-terminus of the Vα chain was as described previously (Wülfing and Plückthun, 1995; Gregoire et al., 1996) (Fig. 1a) with addition of codons for N-terminal methionine and alanine for cloning and expression purposes. The beginning of the Vβ chain was as described (Pircher et al., 1987; Wülfing and Plückthun, 1994), with the N-terminal addition of codons for methionine and aspartate for cloning and expression purposes. An *Nco*I and *Hind*III site were removed from the constant region of the α-chain, and an *Nco*I site was removed from the constant region of the β-chain gene. The unpaired cysteine residue of the Cβ domain was mutated to serine (Fig. 1a, bold), while the C-terminal cysteines were left intact in both chains. An *Nco*I and *EcoR*I site were added to the 5′ and 3′ ends of both genes, respectively, for cloning into the vector pTFT74 (Freund et al., 1993; Ge et al., 1995). The Fos and Jun dimerization domains (Plückthun and Pack, 1997) were added as a *EcoR*I–*Hind*III cassettes to the α- and β-chain, respectively, leading to the final expression plasmids pAT105 and pAT106. The sequence coding for the Fos dimerization domain was obtained from plasmid packn1fosh5 (Pack et al., unpublished) and contained a sequence coding for a his$_5$ tag, while the sequence coding for the Jun domain, obtained from plasmid packn1jun, did not contain any tag. Both Fos and Jun domains

a α-subunit

```
  |start
MAQQKEKHDQQQVRQSPQSLTVWEGGTTVLTCSYEDSTFNYFPWYQQFPG
                                  CDR1

EGPALLISILSVSDKKEDGRFTTFFNKREKKLSLHIIDSQPGDSATYFCA
           CDR2

                      |C-domain
ALYGNEKITFGAGTKLTIKPNIQNPEPAVYQLKDPRSQDSTLCLFTDFDS
   CDR3

QINVPKTMESGTFITDKTVLDMKAMDSKSNGAIAWSNQTSFTCQDIFKET

           |hinge    |Fos coiled-coil
NATYPSSDVPCGGEFGPSGNELTDTLQAETDQLEDKKSALQTEIANLLKE

          |
KEKLEFILAAHHHHH
```

β-subunit

```
  |start
MDEAAVTQSPRSKVAVTGGKVTLSCHQTNNHDYMYWYRQDTGHGLRLIHY
                                CDR1

SYVADSTEKGDIPDGYKASRPSQENFSLILELASLSQTAVYFCASSDAGG
     CDR2                                      CDR3

                |C-domain
RNTLYFGAGTRLSVLEDLRNVTPPKVSLFEPSKAEIANKQKATLVCLARG

FFPDHVELSWWVNGKEVHSGVSTDPQAYKESNYSYSLSSRLRVSATFWHN

                                          |hinge
PRNHFRCQVQFHGLSEEDKWPEGSPKPVTQNISAEAWGRADCGGEFPSGN

  |Jun coiled-coil
EARIARLEEKVKTLKAQNSELASTANMLREQVAQLKQKVMNY
```

b

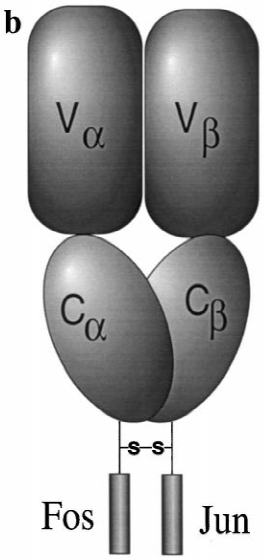

Fig. 1. (a) Amino acid sequences of the expressed α- and β-chains of the TCR P14. The Vα gene segment is of the Vα2, and the Vβ gene segment of the Vβ8.1 gene family. The free cysteine at position 183 in Cβ was mutated to serine, which is in boldface in the sequence. The complementarity determining regions (CDRs, represented in boldface and underlined) were assigned as described by Kabat et al. (1991). The Fos coiled-coil was added to the α-chain construct, while the Jun coiled-coil was added to the β-chain construct. N-terminal methionines were added for bacterial cytoplasmic expression. (b) Schematic representation of the TCR with its Fos and Jun additions. The two subunits contain the cysteines at the end of the extracellular part of the constant domains, which is depicted in this drawing by the dash connecting the two chains.

were connected to the TCR by a spacer region, EFGPSGNE and EFPSGNEA, respectively. The nucleotide sequence of the α- and β-chains were confirmed by sequencing, and the protein sequences are shown in Fig. 1a. A schematic depiction of the domains of the receptor is given in Fig. 1b.

The α-chain of the UZ TCR, without a cysteine at the C-terminus of the α chain (Pecorari et al., 1999) was cloned into the vector pAT105 as an *Nco*I–*Eco*RI fragment, in front of the sequence coding for the Fos domain. The β-chain (Pecorari et al., 1999), also without the C-terminal cysteine at the end of Cβ, was cloned as an *Nco*I–*Eco*RI fragment into a variant of the pAT106 vector, containing a sequence

coding for a his_6 tag at the end of the Jun domain. This sequence coding for a his_6 tag was added by cloning a *Bgl*I–*Blp*I fragment of packihjunh6 into packn1jun, and subcloning it as an *Eco*RI–*Hind*III fragment into pAT106.

A 5′ *Nco*I and a 3′ *Eco*RI site were added to the H-2D^b gene by PCR amplification for cloning into the plasmid pKK74PCLbiot37 (K.M. Müller, unpublished), a derivative of pTFT74 containing a sequence coding for the following biotinylation tag (Schatz, 1993), LHDFLNAQKVELYPVTS. Between the MHC and the biotin tag a spacer of the sequence ASGAEF was encoded. The biotin tag sequence is coded as an *Eco*RI–*Hind*III cassette (K.M. Müller, unpublished). The nucleotide sequence of the H-2D^b gene was confirmed by sequencing.

2.3. Expression of the proteins for inclusion body formation

The expression plasmids were cotransformed with the plasmid pUBS520 (Brinkmann et al., 1989), encoding an arginine-specific tRNA to overcome the problem of rare arginine codons, into the *E. coli* strain BL21(DE3)pLysS as an expression host (Studier et al., 1990). Cells were grown in 1 l of SB medium containing 1% (w/v) glucose, 100 μg/ml ampicillin, 35 μg/ml kanamycin and 15 μg/ml chloramphenicol up to late logarithmic phase (A_{550} = 1–1.2) at 37°C, and induced with 1 mM isopropyl β-thiogalactoside (IPTG). After 4 h of induction, cells were harvested and pelleted by centrifugation. They were resuspended in about 30 ml of 20 mM Tris–HCl, pH 8, briefly sonicated on ice to reduce viscosity, and further lysed with a French press. The lysate was then treated with 1% Triton X-100 and stirred for 30 min on ice. The inclusion bodies were then pelleted by centrifugation for 10 min at 39 000 *g*, washed twice with 20 mM Tris–HCl, 20% (w/v) sucrose, 2 mM EDTA, pH 8.0, and stirred for 2 h at RT (room temperature) in a solubilization buffer containing 6 M (Gdn–HCl), 100 mM Tris–HCl, pH 8.0 and 25 mM dithiothreitol (DTT). The solubilized inclusion bodies were then centrifuged at 39 000 *g* for 10 min, and stored at −70°C. Concentrations were estimated by sodium dodecylsulfate-polyacrylamide gel electrophoresis (SDS–PAGE), by comparison with dilutions of known quantities of marker proteins.

2.4. Refolding and purification of the TCRs

2.4.1. Refolding of the UZ TCR

Expression, refolding and purification of the UZ TCR was performed as described (Pecorari et al., 1999).

2.4.2. Refolding of the P14 TCR by multi-step dialysis

Solubilized inclusion bodies (10 mg/ml) of the two chains were combined by diluting each to 1 μM into a buffer containing 6 M Gdn–HCl, 100 mM Tris–HCl, 2 mM EDTA, pH 8.0, at 4°C, and dialyzed overnight against 20 volumes of 3 M Gdn–HCl, 100 mM Tris–HCl, 2 mM EDTA, 0.2 mM reduced L-glutathione, pH 8.0, at 4°C. All subsequent dialysis–refolding steps were against 20 volumes of buffer. The dialysis buffer was changed to a buffer containing 2 M Gdn–HCl, 100 mM Tris–HCl, 2 mM EDTA, 0.2 mM reduced L-glutathione, pH 8.0, at 4°C, and dialysis continued overnight. The third dialyis step was against a buffer containing 1 M Gdn–HCl, 100 mM Tris–HCl, 2 mM EDTA, 0.37 mM oxidized L-glutathione, 0.37 mM reduced L-glutathione, pH 8.0, at 4°C, overnight. The fourth step was against a buffer containing 0.4 M arginine, 100 mM Tris–HCl, 2 mM EDTA, pH 8.0, at 4°C, overnight. Finally, the protein was dialyzed against TBS, pH 8.0, at 4°C, overnight. The protein was then treated with N-ethylmaleimide of a final concentration of 45 mM for several hours at 4°C. It was then extensively dialyzed against TBS, and concentrated, so that the maximal concentration of the protein did not exceed 400 μg/ml.

2.4.3. Refolding of the P14 TCR by one-step dialysis

For this purpose, the two chains were combined by diluting each to 1 μM into a buffer containing 6 M Gdn–HCl, 100 mM Tris–HCl, 2 mM EDTA, pH 8.0, at 4°C, and dialyzed overnight against 20 volumes of a buffer containing 0.4 M arginine, 100 mM Tris–HCl, 2 mM EDTA, pH 8.0, at 4°C,

overnight. The protein was then dialyzed against TBS, and concentrated.

2.4.4. Refolding of the P14 TCR by dilution

Refolding of the protein was initiated by 100-fold dilution of a solution, containing equimolar amounts of both chains in 6 M Gdn–HCl, into a refolding buffer containing 1 M arginine, 100 mM Tris–HCl, 2 mM EDTA and either 6.3 mM reduced and 3.7 mM oxidized L-glutathione, or 0.2 mM reduced and 0.2 mM oxidized L-glutathione, to give a final concentration of 1 μM of each chain. The proteins were then dialyzed against TBS.

The P14 TCR, refolded by either method, was purified by three runs over a Superdex G200 (Pharmacia) gel filtration column. Fractions were pooled and concentrated after each run, so that the maximal concentration of protein did not exceed 400 μg/ml. Heterodimer containing fractions were identified by reducing and non-reducing SDS–12% PAGE as described in Results. The concentration of the α- and β-chain was determined by spectrometry, using extinction coefficients at 280 nm of 26,330 $M^{-1}cm^{-1}$ and 49,800 $M^{-1}cm^{-1}$, respectively, calculated from their sequences according to Gill and von Hippel (1989).

2.5. Expression and purification of the BirA protein

The expression plasmid for the BirA protein (K. Brandt and K.M. Müller, unpublished) was transformed into the *E. coli* strain BL21(DE3)pLysS, and grown in SB medium containing 100 μg/ml ampicillin, 15 μg/ml chloramphenicol at 30°C up to mid-logarithmic phase ($A_{550}=0.6$). The cells were then induced with 1 mM IPTG, and grown for another 3 h. They were then harvested, centrifuged and finally resuspended in 20 mM Tris–HCl, pH 8.0. They were briefly sonicated on ice to reduce viscosity, and further lysed with a French press. The lysate was centrifuged at 39 000 *g* for 10 min, and passed through a 0.22-μm filter. Purification was performed first on a BioCAD 60 system (PerSeptive Biosystems Cambridge, MA, USA) by immobilized metal affinity chromatography on a Poros 20 IDA column, and then by cation-exchange chromatography, on a Poros 10 S/H column, at pH 7.3.

2.6. Preparation of the H-2D^b complexes

The complexes, consisting of peptide, H-2D^b, and β_2-microglobulin were refolded as described (Pecorari et al., 1999) and purified by anion-exchange chromatography on the BioCAD system with a Poros 20 HQ column, using a step gradient of NaCl. The complexes of the biotin-tagged heavy chain were produced and purified identically.

2.7. Biotinylation of the tagged complexes and tetramerization

The complexes were biotinylated essentially as described (Altman et al., 1996). The H-2D^b complex was biotinylated at 5 μM in a buffer containing 50 mM Tris–HCl, 5 mM ATP, 100 μM biotin, 5 mM $MgCl_2$ and 5 μM BirA, pH 7.5, overnight at RT without stirring. The biotinylated protein was extensively dialyzed against TBS to remove the free biotin, and concentrated to 12–16 μM. It was mixed at a ratio of 4:1 with a neutravidin–horseradish peroxidase conjugate (Nav–HRP, Pierce, Rockford, IL, USA) and incubated for 1 h to give a complex of, ideally, four pMHCs with Nav–HRP.

2.8. ELISA with tetramers

The anti-Cβ monoclonal antibody H57–597 (Kubo et al., 1989) was coated at 2 μg/ml, 50 μl/well onto Maxisorp ELISA plates (Nalge Nunc, Rochester, NY, USA), in TBS buffer (pH 8.0 at RT) overnight at 4°C or for 2 h at RT with shaking. The plate was washed once with TBS buffer containing 0.05% Tween (TBST buffer) and blocked by adding 5% skim milk in TBST for 1 h at RT. The plate was washed once with TBST, and the TCR was added at concentrations between 0.2 and 2 μg/ml, 50 μl/well, and shaken for 1 h at 4°C. The plate was then washed three times with TBST buffer, and the pMHC-tetramer Nav–HRP complex was added at a concentration of 12.5–50 nM, in 0.25% bovine serum albumin (BSA) in TBST, 50 μl/well. For inhibition experiments, the tetramer solution additionally contained the pMHC monomers at the final concentration indicated in Results. The plate was shaken for 1 h, and then washed three times with TBST and once with TBS as follows. Since the very

weak interaction of TCR and monomeric pMHC could lead to dissociation of the complex after extended washing, one row was washed at a time, by dispensing the liquid with a multipipetter, and removing it again immediately by rapidly inverting the plate, to minimize contact time. At this stage the plate was brought back to RT, and detection was achieved by dispensing 50 μl BM-blue POD substrate (Roche Diagnostics, Rotkreuz, Switzerland) in the wells, and shaking until the signal had developed. The reaction was stopped by adding 125 μl of 0.1 M HCl.

2.9. Surface plasmon resonance

All measurements were performed on a BIAcore instrument (Pharmacia Biosensors, Uppsala, Sweden) at 20°C. The anti-Cβ monoclonal antibody H57–597 (Kubo et al., 1989) (378 μg/ml, 30 mM acetate, pH 4.2) was immobilized on a CM5 sensor chip using the following protocol, with HBS containing 0.005% Tween as the flow buffer. The surface was activated with a 7 min pulse of a 0.1 M EDC–0.05 M NHS mixture (35 μl, 5 μl/min), 20 μl of the anti-Cβ antibody H57–597 were then injected over 4 min, and the surface was finally deactivated by injecting 35 μl of 0.1 M ethanolamine–HCl, pH 8.5. The procedure resulted in about 4800 RUs of antibody bound to the chip. A deactivated control surface was prepared using the same protocol, except that no antibody was injected, but instead the surface was directly deactivated with ethanolamine after activation.

For the determination of the specificity of the TCR P14 interaction with pMHC, the running buffer was TBS, pH 8.0, 0.005% Tween. First, 10 μl of the purified P14 TCR (50 μg/ml) was injected at 5 μl/min over the anti-Cβ monoclonal antibody H57–597 surface, giving a signal of about 650 RUs. The pMHCs (10 μM) were then injected, in 7-μl pulses, in the following order: (the names refer to the peptides, all MHCs are H-2D^b) myhsp60 (non-cognate), gp33 (cognate) and gp276 (non-cognate). The surface was regenerated with 10 μl of 0.1 M glycine–HCl, 500 mM NaCl, pH 2.5, at 30 μl/min, after injection of the three pMHCs. The three pMHCs were then injected over a deactivated control surface, and the final signal was calculated by subtracting the signal obtained on the deactivated surface from the signal on the TCR-containing surface, to remove the contributions of the bulk effect and possible non-specific binding. Each measurement was performed at least twice.

For the measurement of the affinity of the P14 TCR to the cognate pMHC gp33, the running buffer was HBS, containing 0.005% Tween. The procedure was essentially the same, the TCR was first injected on a surface containing the monclonal antibody, followed by injection of the pMHC. The surface was regenerated as above, after each injection. The pMHC was injected on the deactivated surface, which was also regenerated after injection, although the signal returned to baseline level after completion of the injection of pMHC. The signal was again calculated by subtracting the signal obtained on a deactivated control surface from the signal obtained on the TCR surface. Each data point was the average of two measurements. The dissociation constant was obtained by plotting (KALEIDAGRAPH 3.08, Synergy Software, Reading, PA, USA) the signal in RUs against the concentration of the injected pMHC, and fitting to a hyperbolic curve $RU = RU_{max} \cdot [pMHC]/(K_D + [pMHC])$, where RU_{max} is the maximal value at saturation.

3. Results

3.1. Expression and purification of the TCRs

As the association of the TCR α- and β-chain with each other is very weak (Pecorari et al., 1999), the stability of the αβ-heterodimer has long been a problem in production of TCRs (Weber et al., 1992; Chang et al., 1994; Pecorari et al., 1999). While in our previous studies on TCR UZ we found yields of the unmodified and non-disulfide linked αβ-complexes to be higher than any other variant tested, this was not the case for TCR P14. First, we observed the presence of α-homodimers when trying to refold a construct devoid of any dimerization domain, and second, we noticed strong aggregation to high molecular weight species. Therefore, we cloned the α-chain in front of a Fos leucine zipper domain, and the β-chain in front of the Jun leucine zipper domain, to improve chain association and possibly

solubility, since the leucine zippers have a high content of charged residues. The two fusion proteins were produced separately as inclusion bodies, and refolded together in equimolar amounts. A multi-step dialysis method according to Tsumoto et al. (1998) was used, with omission of the last dialysis step from 1 to 0.5 M Gdn–HCl. This sample of P14 TCR, which gave unequivocal results demonstrating its functionality (see below), was then used as a control in testing the efficiency of other refolding methods, and a simpler one-step dialysis method was developed as the optimal procedure (see below).

The protein from multi-step dialysis was then purified by three cycles of gel filtration followed by concentration steps. A peak of molecular weight (M_W) of 82 kD (expected M_W 62 kD) could be isolated after the three successive gel filtration runs (Fig. 2a). An analysis of this peak by both reducing and non-reducing SDS–PAGE is shown in Fig. 2b. As seen from the band in the reducing lane, the two chains are present in approximatively equal amounts in the isolated peak. The non-reducing lane shows that both chains are fully oxidized to a dimeric form. On the other hand, the peak is a heterogeneous mixture of several oxidized species, as can be seen from the diffuse pattern of bands. This had also been observed by Garboczi et al. (1996b), when they refolded the A6 TCR containing the terminal cysteine residues in both chains, albeit by a different method.

While the above experiment could not rigourously exclude the fortuitous presence of an equimolar mixture of α- and β-homodimers, we confirmed by BIAcore that the two chains are actually present in a heterodimeric assembly. This was achieved by binding the TCR first to the anti-Cβ monoclonal antibody H57–597 (Kubo et al., 1989), derivatized on the chip, and subsequently demonstrating the binding of the anti-Vα2 monoclonal antibody B21.5 (Pircher et al., 1992) to the bound TCR (data not shown).

The UZ TCR (Pecorari et al., 1999) was also cloned in the same format, with a Fos domain behind the α-chain, and a Jun domain behind the β-chain. In this case, however, the two chains were cloned

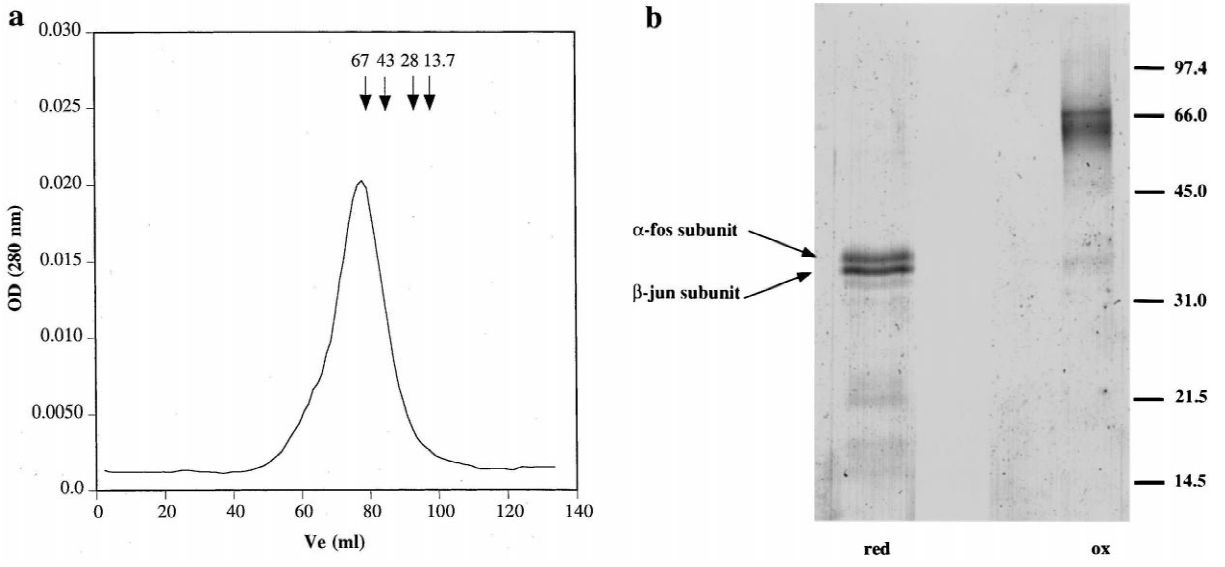

Fig. 2. (a) Gel filtration chromatogram of the P14 TCR. The chromatogram of the third passage over the Superdex G200 (Amersham Pharmacia Biotech, Uppsala, Sweden) is shown. The arrows indicate the molecular weight of the calibration proteins. The peak isolated has a molecular weight of 82 kD (expected 62 kD). (b) The fraction isolated by gel filtration chromatography was analyzed by reducing (red) and non-reducing (ox) SDS–PAGE. The peak contains approximately equimolar amounts of both α- and β-chains, and as seen from the non-reduced sample, contains species migrating at the molecular weight of dimers. The non-reduced sample is heterogeneous, showing that there must be several disulfide-crosslinked species in the sample. The α-chain with the Fos coiled-coil is very acidic, and runs higher than the β-chain with the Jun coiled-coil.

without the C-terminal cysteine. The reason for now using dimerization domains for the UZ TCR was that we wanted to immobilize the receptor for the various assays described below, and we therefore needed the two subunits of the receptor to be stably associated (Pecorari et al., 1999). The expression, refolding and purification of the protein was identical to the previously described method used for the variant without the Jun and Fos domain (Pecorari et al., 1999), albeit with a lower yield for the Jun and Fos fusions. This supports our previous conclusion that overcoming the weak association by linking the two chains may cause aggregation problems during refolding. For TCR P14, however, it seems that the leucine zipper domains, which contain several charged residues, outweigh this disadvantage by contributing to solubility. The mode of refolding could also play a role, since the TCR P14 was refolded by dialysis. It thus appears as if the optimal format and refolding method may not only be dependent on each other, but also on the particular TCR sequence.

3.2. Development of the MHC-tetramer assay

In an effort to simplify and accelerate the analysis of the functionality of recombinant TCRs, we developed an assay based on the tetramerization of the MHC through biotinylation, similar to the method of Altman et al. (1996), used originally for identifying T-cells which recognize a given pMHC complex. The goal was to be able to analyze several samples in parallel, and we turned therefore to an ELISA format. The need for tetramerizing the MHC was given by the very weak dissociation constants (K_D) of the TCR–pMHC interactions (reviewed in Davis et al., 1998). They are mostly between 10^{-4} and 10^{-6} M, with the exception of an allogeneic pMHC–TCR interaction reported to be of higher affinity. The experience in our laboratory has been that enzyme-linked immunosorbent assay (ELISA) assays do not work reliably for monovalent antibody fragments when the dissociation constant is worse than 10^{-6} M (Pack and Plückthun, 1992), as would be expected from simple equilibrium and off-rate considerations.

A schematic description of the assay is shown in Fig. 3a. A neutravidin–HRP conjugate was chosen for building the tetramer and to allow for detection. Coating of the TCR was achieved indirectly by first coating the anti-Cβ monoclonal antibody H57–597, and subsequently binding the TCR to it at 4°C. This was done as to maximize functionality of the TCR and allow for productive orientation of the TCR on the plate. We indeed found a dramatic improvement in signal when comparing the indirect TCR coating to an ELISA performed with direct coating of the TCR (data not shown). Our concern was to reach a high enough density of potentially active TCR molecules in order to allow for multimeric pMHC binding to occur.

Biotinylation of the MHC was carried out as described by Altman et al. (1996). To the C-terminus of the heavy chain H-2D^b was fused a cassette encoding a spacer and a biotin tag. The tagged heavy chain was refolded as described for the untagged heavy chain, and purified under the same conditions, followed by enzymatic biotinylation. Multimerization of the biotinylated pMHC monomers with neutravidin–HRP was achieved by mixing the two components in a 4:1 molar ratio with the biotinylated pMHC and neutravidin–HRP at final concentrations of 13–14 μM, or 3.2–3.5 μM, respectively.

The efficiency of complex formation and of biotinylation was assessed by SDS–PAGE in two ways. We made use here of a property of avidin and streptavidin to not dissociate into monomers upon SDS treatment (Bayer et al., 1996), if not heated above 50°C. When the complex was formed with an excess of streptavidin over pMHC, no protein remained at the size of the monomeric biotinylated pMHC, indicating that all pMHCs are engaging in complexes with neutravidin and thus full biotinylation must have occurred (data not shown). Furthermore, complex formation with Nav–HRP was tested by forming the complex at a 4:1 ratio, and separating the uncomplexed from the complexed pMHC monomers by ultrafiltration with a concentrator of M_W cut-off of 100 kD, through which pMHC was shown to be able to pass (data not shown). The filtrate and the supernatant were analyzed by SDS–PAGE, and the absence of a band at the monomer size in the filtrate indicated that complex formation was complete.

As the neutravidin in the neutravidin–pMHC tetramers was already conjugated to horseradish peroxidase, it could be directly detected by using a

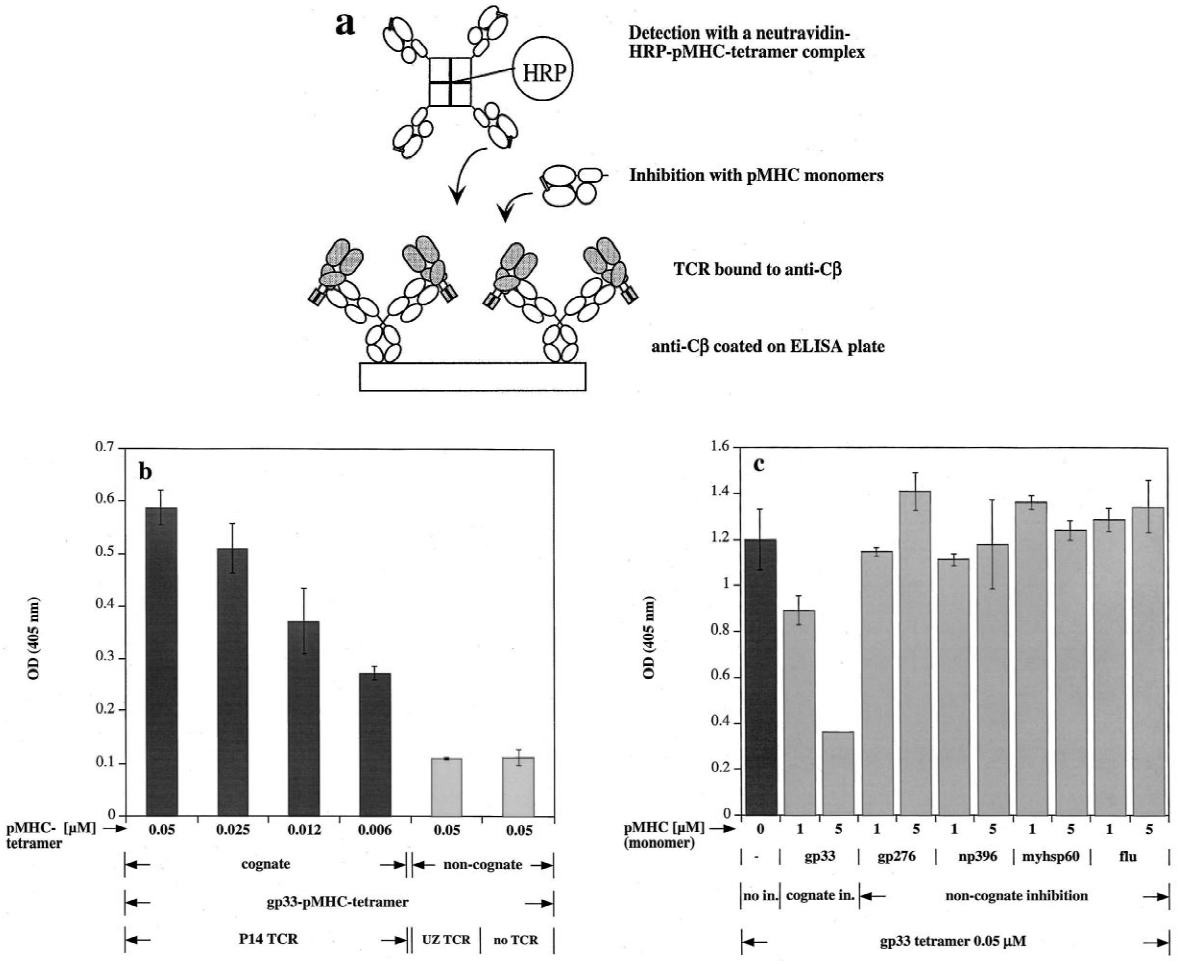

Fig. 3. (a) Schematic representation of the tetramer ELISA assay. The assay detects binding of tetrameric pMHC bound to TCR, indirectly coated to an ELISA plate through the anti-Cβ monoclonal antibody H57–597. Detection is achieved by reaction with a peroxidase substrate. The assay is performed with or without inhibition with soluble monomeric pMHC. (b) The TCRs were bound to an ELISA plate coated with the H57–597 anti-Cβ monoclonal antibody. The tetramers were then added, and after washing, binding was detected with a peroxidase substrate. The numbers below the bar graph indicate the concentration of the tetramer. The cognate pMHC of the P14 TCR is the gp33-pMHC, which is not recognized by the UZ TCR. As seen in this graph, the signal of the tetramers with the cognate TCR is dose-dependent. Two additional controls are shown in this experiment. First, the tetramers do not give any signal in the absence of TCR, and second, there is no interaction between a non-cognate TCR and the gp33-tetramer. (c) Inhibition assay, where the tetramers are added in the presence of two concentrations of cognate and non-cognate monomeric pMHCs as inhibitors of the interaction of the tetramers with the TCR. The signal of the gp33-tetramer can only be inhibited by the cognate gp33-monomer, and not by the non-cognate pMHC monomers. The numbers below the chart bars indicate the inhibitor concentration in μM. The first bar (darker) shows the signal without inhibition. The P14 TCR was bound to the plate at a concentration of 1.7 μg/ml through its interaction with the anti-Cβ monoclonal antibody H57–597 and detection was achieved in all cases with a tetramer concentration of 0.05 μM.

peroxidase substrate. This had the further advantage of avoiding additional washing steps which would be necessary when using, for example, a two-step detection system with a monoclonal antibody followed by a second antibody conjugated to HRP for detection.

The result of a tetramer binding experiment is shown in Fig. 3b. As can be seen, the signal is

dependent on the concentration of pMHC-tetramers. Furthermore, there is no signal above background when a non-cognate TCR, the UZ TCR, is bound to the plate via the anti-Cβ antibody instead of the P14 TCR. Likewise, no signal above background is seen in those wells where the P14 TCR is bound, but detection is attempted by using a tetramer of the pMHC containing the non-cognate myhsp60 peptide instead (data not shown) (Pecorari et al., 1999). The tetramers also do not bind non-specifically to the anti-Cβ monoclonal antibody H57–597 in the absence of any TCR bound to the plate (Fig. 3b).

Interactions taking place on surfaces can be due to many artefacts, and although the criteria of recognition of only the cognate TCR on the one hand, and no recognition by a non-cognate pMHC tetramer on the other hand, are quite stringent, we chose to apply an even more stringent test to our system. We thus measured the inhibition of the interaction between the tetrameric pMHC complex and the TCR bound to the plate by monomers of various pMHC complexes, containing different peptides. As shown in Fig. 3c, of the five pMHC tested, only the cognate monomeric gp33-pMHC is able to inhibit the signal of the gp33-pMHC tetramers at 5 μM concentration. Inhibition is concentration dependent, and this further demonstrates the specificity of the interaction, since the various pMHCs differ only in their displayed peptide, the heavy chain H-2D^{b} being identical.

3.3. Functionality test of the TCR using BIAcore analysis

The use of tetrameric pMHCs in an ELISA type assay thus allowed us to demonstrate the functionality of our refolded TCR. We decided to use a different method of analyzing the interaction between the TCR and its cognate pMHC as an additional control. Surface plasmon resonance using biosensors has been already used successfully for a number of TCR–pMHC interactions (Corr et al., 1994; Matsui et al., 1994; Alam et al., 1996; Lyons et al., 1996; Pecorari et al., 1999). We chose to immobilize the TCR to the surface through the anti-Cβ antibody, in order to minimize the heterogeneity of the surface. In addition, the pMHC is stable at very high concentration in the injected solution, which is also of advantage when investigating interactions of very low affinity. The TCR was injected onto the surface, and bound to the antibody (Fig. 4a). The pMHC complexes were in turn injected after an equilibration time of 100 s. The non-cognate pMHC containing the myhsp60 peptide, recognizing the UZ-TCR, was always injected first, followed by the cognate pMHC containing the gp33 peptide and another non-cognate pMHC, containing the gp276 peptide. The antibody surface was then regenerated, and the pMHCs were injected on a inactivated naked sensor lane. The specific signal of each pMHC on the TCR surface was obtained as the difference of the signal on the TCR subtracted from the signal on the uncoated lane, consisting of the bulk effect of the protein and possible non-specific interactions with the sensor matrix. Each experiment for obtaining such a sensorgram was repeated at least twice. The background-corrected sensorgrams are shown in Fig. 4b. The two non-cognate pMHCs containing myhsp60 and gp276 do not interact with the TCR P14, and the signal produced by these pMHCs is identical on a P14 TCR surface and on an uncoated inactivated surface. The cognate pMHC containing gp33, however, gives a strong specific signal on the TCR P14, showing that there is a significant fraction of functional protein in the peak isolated by gel filtration.

We ruled out any interaction between the pMHC containing gp33 and the anti-Cβ monoclonal antibody H57–597, by testing this pMHC on the freshly regenerated antibody surface, which produced a signal identical to the signal obtained on the inactivated surface (data not shown). The plateau shape of the curve indicates a rapid equilibration of the molecules on the surface (Plaksin et al., 1997; Pecorari et al., 1999). As we can see from Fig. 4b, the subtraction of the trace obtained on the control surface from the one obtained on the TCR surface yields a nearly rectangular binding curve. The off-rate of the interaction between the P14 TCR and the gp33 pMHC is thus within the range of the dead time of the instrument when injecting pMHC. We estimated a value of about 0.5 s^{-1} at a flow-rate of 30 μl/min for the off-rate, by fitting the dissociation part of the binding trace (data not shown). These fast kinetics are however a superimposition of the mixing process of the instrument and the real kinetics, and therefore contain large errors. Dissociation rate con-

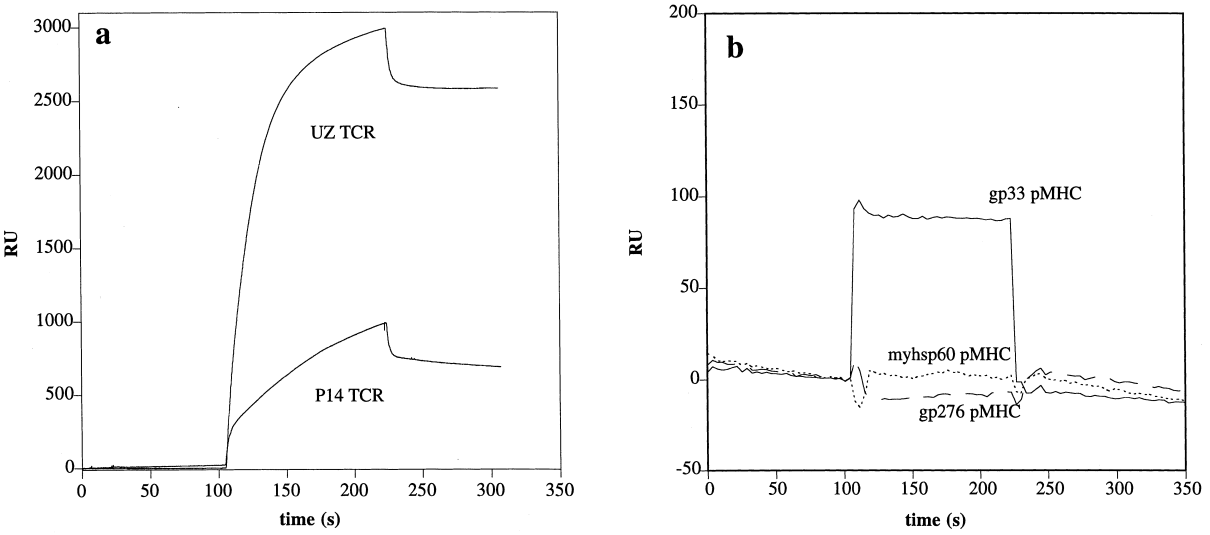

Fig. 4. (a) Binding of the P14 and UZ TCRs at a concentration of 50 μg/ml to the anti-Cβ monoclonal antibody H57–597 derivatized on a BIAcore chip, detected by SPR. The binding curves obtained with the UZ TCR and P14 TCR are labeled accordingly. The two surfaces used in the experiment had the same amount of anti-Cβ monoclonal antibody derivatized, as judged by the resulting amount of RUs coupled. The measurements were repeated several times, and the surfaces could be regenerated with 100 mM glycine HCl, pH 2.5, 500 mM NaCl. (b) Sensorgrams of the binding of the cognate pMHC, gp33, and two non-cognate pMHCs (gp276 and myhsp60) to the P14 TCR. The TCR was bound to a sensor chip derivatized with the anti-Cβ monoclonal antibody H57–597. Each pMHC was also injected over a blank inactivated surface, and this signal was subtracted from the signal obtained on the TCR surface, to remove contributions from the bulk effect and potential unspecific binding. The non-cognate and cognate pMHCs differ only in the peptide they are harboring, the heavy chain being the same (H-2D^b). The solid line represents the signal of the cognate pMHC gp33, the dashed line the signal of the non-cognate pMHC gp276, and the dotted line the signal of the non-cognate pMHC myhsp60.

stants within this range have also been found for high affinity TCRs recognizing class-I pMHCs (Ding et al., 1999; Willcox et al., 1999). The isolated P14 TCR thus recognizes the cognate peptide gp33 in the context of the MHC molecule H-2D^b, but not the two other peptides gp276 or myhsp60 in the context of the same MHC molecule, proving the specificity of the interaction.

A comparison of the association phase obtained by injecting the P14-TCR and the UZ-TCR at the same total concentration on an anti-Cβ antibody surface of the same coating density (Fig. 4a) illustrates the heterogeneity of the P14 TCR preparation. The indirect coupling of the TCR to the surface of the sensorchip via the anti-Cβ monoclonal antibody H57–597 is thus a functional purification step, presumably enriching for correctly folded and associated TCR molecules.

3.4. Using the tetramer assay to optimize folding

With an easy and fast assay now available, we decided to directly compare three different refolding methods. Two of them have been published (Garboczi et al., 1996b; Pecorari et al., 1999), and are based on the dilution of the protein into a non-denaturing buffer, while the third one is a multi-step dialysis method, which we adapted from a published refolding method for antibody fragments (Tsumoto et al., 1998). The three methods were performed in parallel, using equal amount of protein at the start, and leaving the protein to refold for the same amount of time. The crude refolding mixtures obtained by the three methods were analyzed by the tetramer ELISA in parallel, using a dilution series. The protein from the three refolding mixtures was diluted to the same theoretical value before performing the

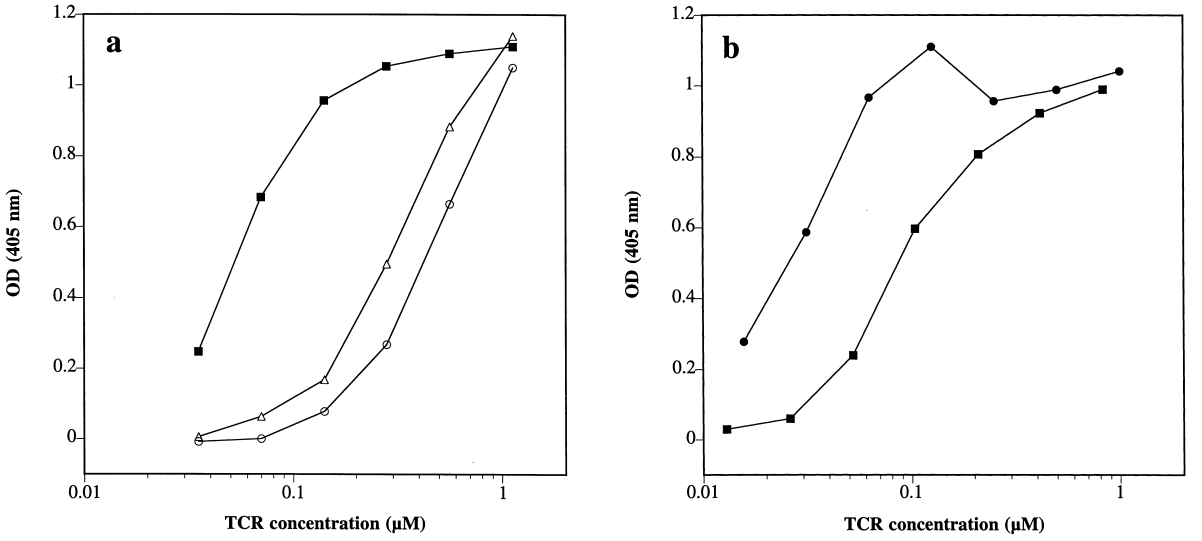

Fig. 5. (a) The efficiency of three refolding methods was compared using the tetramer ELISA assay. Refolding was performed at the same protein concentration in all three cases, and volumes were kept identical. The *x*-axis indicates the concentration of TCR applied to the wells, calculated assuming the absence of any protein loss during refolding. The filled squares show the result of the multi-step dialysis method (details in the text). The open triangles show the result of a dilution–refolding method, with a redox shuffle of 6.3 and 3.7 mM reduced and oxidized L-glutathione, respectively. The open circles show the result of a dilution–refolding method where the redox shuffle contains equimolar concentrations (0.2 mM) of reduced and oxidized L-glutathione. The multi-step dialysis refolding method produces about five times more active protein than the dilution methods. (b) Comparison of the efficiency of refolding of the one-step dialysis method with that of the multi-step dialysis method. The *x*-axis indicates the concentration of TCR applied to the wells, calculated assuming the absence of any protein loss during refolding. The filled circles show the result of the one-step dialysis method, while the filled squares show the result of the multi-step dialysis method. The one-step dialysis method produces about three times as much functional protein as the multi-step method.

ELISA, such that the total protein concentration in the three mixtures would be equal in the absence of aggregation or other protein loss. The refolding mixtures were centrifuged before performing the ELISA test.

As shown in Fig. 5a, the multi-step dialysis method performs best, giving about five times as much functional protein as the two other methods, when comparing the signals in the linear domain of the plot below saturation. Interestingly, the amount of total protein (not shown) parallels the functional protein (Fig. 5a), indicating that the two dilution methods lead to loss of total protein by aggregation, but do not produce more soluble misfolded molecules than the multi-step dialysis method. This is strongly suggestive of an early aggregation step that would be prevented by the more gradual approach towards native conditions, as occurring in the multi-step dialysis method.

We also compared a more straightforward one-step dialysis with the multi-step dialysis method. In this procedure, the protein is dialyzed directly against a native refolding buffer, in the absence of added redox reagents in the refolding buffer. The results are shown in Fig. 5b. Clearly, for this TCR, the one-step approach has a higher yield than the multi-step approach described above, which in turn had been the best of the published methods. Furthermore, the derivatization with maleimide, which is necessary for the multi-step approach to prevent disulfide rearrangements occurring upon concentrating the protein, is avoided. We could also inhibit the ELISA signal for the protein produced by the one-step dialysis method specifically with the cognate, but not with an irrelevant pMHC (data not shown). We thus used this method for the further experiments.

Structural characterization of TCR–pMHC interactions, and possibly bigger complexes, remain one

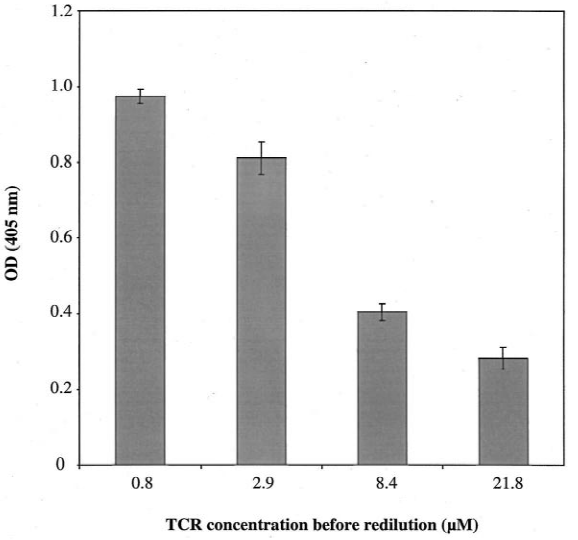

Fig. 6. Stability to concentration. Purified P14 TCR was increasingly concentrated to the values indicated, up to 1.36 mg/ml. The samples were then rediluted to the original volume before concentration, which was the same for all samples, and analyzed by tetramer ELISA. The number below each bar stands for the concentration of the TCR in μM reached in the concentration step prior to redilution. If the TCR could be concentrated with no loss, a constant signal would be expected.

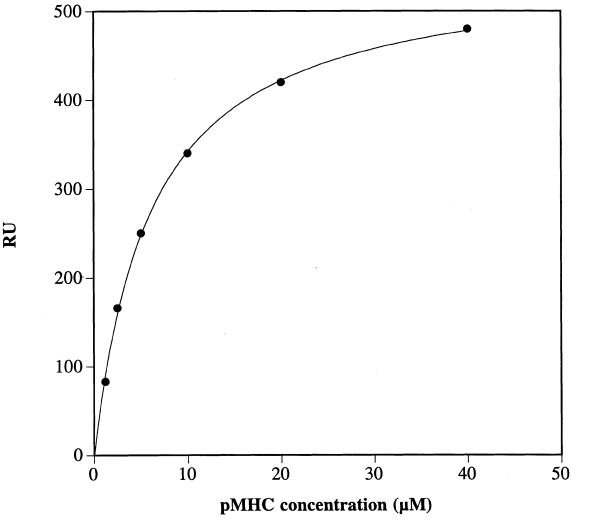

Fig. 7. Measurement of the dissociation constant (K_D) of the gp33-pMHC for the immobilized P14 TCR by SPR with the BIAcore (Pharmacia Biosensors). The TCR was bound on the anti-Cβ monoclonal antibody H57–597 immobilized on a CM5 sensorchip. The pMHC was first injected on the TCR surface and then over a blank inactivated surface. The signal over the blank surface was subtracted from the signal obtained on the TCR to eliminate the contribution of the bulk effect and of possible unspecific binding to the dextran matrix of the sensorchip. The surfaces were regenerated after each injection, and new TCR was injected for each run. K_D was obtained by fitting a hyperbolic curve to the plot of the BIAcore signal in RUs against the concentration of injected pMHC. The value obtained was 6 μM.

of the challenging questions in immunology, and for this purpose highly stable receptors are required. We thus investigated the ability of our receptor to be concentrated. For this experiment, we first concentrated the protein, and then diluted again the various concentrations of TCR to an identical final theoretical concentration, and analyzed the signal by tetramer ELISA. A constant signal would mean that the protein is not precipitating upon concentration. As seen in Fig. 6, however, the intensity of the signal strongly decreases if the protein is concentrated above 2.9 μM. The P14 TCR is thus unstable when concentrated.

3.5. Determination of the binding constant of the P14 TCR by SPR

We chose the same BIAcore coupling strategy as above to measure the dissociation constant (K_D) between the P14 TCR and its cognate pMHC, the gp33 pMHC. We first bound the receptor to the anti-Cβ antibody-coated chip, and then injected the pMHC. The surface was regenerated with a glycine buffer of a low pH, and the pMHC was injected over a blank, inactivated surface to obtain a control value for the bulk effect. The measurements were carried out in duplicate for several concentrations, and the response for each concentration was calculated by subtracting from it the signal obtained on the blank surface, and averaging over at least two measurements. The result is shown in Fig. 7. The K_D value obtained for the P14 TCR of 6 μM indicates that it is in the upper range of affinities measured so far for these receptors (reviewed in Davis et al., 1998).

4. Discussion

4.1. Performance of the assay

Assays for detecting the expression and functionality of T-cell receptors at small scales or in crude

mixtures have so far relied on antibodies, some of which recognize conformational epitopes. Antibodies have the advantage of being very specific and generally of high affinity, thus allowing sensitive detection of molecules in crude extracts during expression (Wung and Gascoigne, 1996). There are, however, very few antibodies which have epitopes encompassing both the Vα and the Vβ domain of the same TCR (Sykulev et al., 1994), and most if not all of the so-called conformationally specific antibodies also recognize TCRs in non-reducing Western blots (Schodin et al., 1996), and thus cannot a priori be considered a proof of functionality. Instead, they may already give positive signals when partial folding has occurred and possibly in the absence of the correct Vα–Vβ interaction.

We have used our tetramer assay to detect functional TCRs in crude refolding mixtures by directly measuring the interaction with pMHC. We were able to use tetramer concentrations as low as 10 nM to detect the functional TCR at concentrations of less than 16 nM. The sensitivity of the assay will certainly be dependent on the intrinsic affinity of the particular pair of TCR monomer and pMHC monomer for each other, but in principle, even the low affinity TCRs should be recognized, as both the density of coating of the receptors and the concentration of the tetramers can be further increased. The assay is also not limited to TCRs refolded from *E. coli*, since proteins from any type of supernatants can be captured in the initial step.

The ability of the assay to detect proteins from the crude refolding extract is also essential for isolating receptors of low stability, since these may aggregate upon concentration, a step usually needed for the purification of the TCRs (Garboczi et al., 1996b; Plaksin et al., 1997; Pecorari et al., 1999). Indeed, we would not have been able to characterize the P14 TCR, had we concentrated the protein too much (Fig. 6).

4.2. Refolding of recombinant TCRs

Early aggregation (Buchner and Rudolph, 1991; Kiefhaber et al., 1991), has long been recognized as one of the major side reactions limiting the yield of refolding of proteins. To circumvent this problem, a series of strategies have been developed (Buchner et al., 1992; Kurucz et al., 1995; Maeda et al., 1996; Rozema and Gellman, 1996; Rudolph and Lilie, 1996; Stempfer et al., 1996; Tsumoto et al., 1998) which, however, have not proven to be general, and so they have to be optimized for each protein. For the TCR and other heterodimeric proteins, chain pairing has also been recognized as one of the limiting factors (Chang et al., 1994; Scott et al., 1996; Pecorari et al., 1999). The use of association domains (Pack and Plückthun, 1992; Plückthun and Pack, 1997; Müller et al., 1998), such as the Jun and Fos domains, or the immunoglobulin constant domains have been used to circumvent this with some success (Traunecker et al., 1989; Chang et al., 1994; Scott et al., 1996). We have now found evidence for a third bottleneck on the way to refolded TCRs, namely the stability of the native receptor.

We have produced our TCR as a fusion to the Fos and Jun domains for the α- and the β-chains, respectively, and have kept the terminal cysteines in the constant domains, which did oxidize in the refolding procedure to an intermolecular disulfide bridge as evidenced in Fig. 2a. Chain pairing thus does not seem to be a limitation in the present constructs. Expression of the two chains in *E. coli*, however, produces unglycosylated protein, and this might conceivably be affecting stability, as has been shown for several proteins (Wang et al., 1996), notably for CD2 (Withka et al., 1993), or ribonuclease B (Joao et al., 1992). On the other hand, numerous other examples are known where glycosylation does not affect stability (Powell and Pain, 1992; Tams and Welinder, 1998). In the crystal structure of the glycosylated 2C TCR (Garcia et al., 1996), there is a large ordered carbohydrate stretch involved in the Cα–Cβ interaction. Although several receptors have now been successfully produced from *E. coli* (Garboczi et al., 1996b; Golden et al., 1997; Pecorari et al., 1999), it is conceivable that for some receptors of lower intrinsic stability, the lack of these interactions would be enough to decrease stability such that they cannot be isolated at high concentration. Alternatively, the stability of the receptor might be sufficient for fulfilling its function in the cellular context. The chains of the coreceptor CD3, which are part of the TCR complex on the cell surface, might also provide stabilization. Finally, it is

possible that anchoring of the receptor in the membrane could be sufficient to prevent aggregation.

4.3. Affinity and activity of TCRs in vivo

The successful production of soluble and functional recombinant P14 TCR allows us to compare in vitro interaction data between the gp33-pMHC and P14 TCR, obtained in this study, with in vivo data on this T-cell response and the response of other T-cells in the mouse upon infection with the lymphocytic choriomeningitis virus (LCMV).

To correlate affinities, measured between soluble TCRs and pMHCs, and cytotoxicity at the level of the cytotoxic T-cells, one has to assume that the interaction between cell-bound receptors taking place at the cell–cell interface can be described by the law of mass action, albeit in the more complicated context of mobile, cell bound molecules (Sykulev et al., 1995). The free concentrations of the interacting pMHC and TCR have to be replaced by their density at the surface of the antigen presenting cells (APCs), and T-cells, respectively. Gallimore et al. (1998a) have found the peptide gp33 to be the most abundant of the three major epitopes of LCMV when eluting peptides from H-2D^b molecules purified from LCMV-infected MC57 cells. They found that this epitope was about seven and twelve times more abundant than the epitopes gp276 and np396, respectively. The magnitude of the T-cell response stimulated after virus infection for each of these epitopes followed the same order. In cytotoxic assays using cell lines generated with APCs pulsed with the peptide gp33, or np396, respectively, half-maximal lysis however occurs only at a 1000-fold higher concentration of the peptide gp33 than of np396 (Gallimore et al., 1998a). Likewise, T-cells elicited against the np396 epitope are much more efficient at clearing virus in adoptive transfer experiments (Gallimore et al., 1998a). No difference in the level of TCR expression between the T-cell lines specific for the three epitopes was found (Gallimore et al., 1998a), and it could be thus argued that the affinity of the TCRs of the gp33-specific T-cell clones might be, on average, much lower than the affinity of the np396 T-cell clones. We have measured the affinity of the P14 TCR for the gp33-pMHC, and have obtained a K_D of 6 μM, close to the highest values found for the affinity of syngeneic TCR–pMHC interactions of 2 μM (Sykulev et al., 1994). However, we cannot rigorously exclude that some of the other peptides might elicit T-cell responses with unusually high affinity, and the final interpretation will have to wait for the K_D determination of the other pMHC–TCR complexes as well. The P14 T-cell clone is quite representative of gp33-specific polyclonal T-cell lines, and the dose–response curve of cytotoxicity or activation in dependence of the peptide concentration is the same as the average dose response curve obtained with the T-cell line, within the experimental deviation of such assays (Ohashi et al., 1993; Bachmann et al., 1996; Oxenius and Bachmann, 1997; Gallimore et al., 1998a). It will thus be interesting to compare directly the P14 T-cell clone and the polyclonal T-cell line for the level of expression of coreceptors such as CD8. This will help to clarify whether it is the affinity of the receptors of the T-cell line or the level of expression of coreceptors that are responsible for the dramatic difference in dose–response curves between the gp33- and the np396-specific T-cell lines. Alternatively, the difference in dose–response of the cell lines might be explained by differences in the kinetics of recognition (Matsui et al., 1994; Davis et al., 1998) that would be affecting signalling through the TCRs. The correlation of these in vivo data with direct measurements of the isolated molecules, greatly facilitated by the methods described in the present study, will be decisive to describe T-cell activation at the molecular and structural level.

5. Conclusions

We have developed a method to rapidly identify and quantify functional soluble T-cell receptors on a microscale, which should be independent of the expression system used. This has allowed us to isolate an unstable T-cell receptor and characterize its binding to its cognate pMHC. The signal could be detected in a highly sensitive manner, and was shown to be specific, and could be confirmed by BIAcore measurements. We believe that this method should accelerate the characterization of TCR–pMHC interactions, and generally broaden the scope

of receptors amenable to biophysical characterization.

Although unstable receptors are not yet suitable for structural characterization, our method allowed us to identify the functionality of the receptor already in an early part of the characterization, allowing thus future optimization of stability. Several such protein engineering approaches for improving folding and expression have been published (Knappik and Plückthun, 1995; Jung and Plückthun, 1997; Patten et al., 1997; Crameri et al., 1998; Giver and Arnold, 1998; Proba et al., 1998), and it should become feasible to rescue these receptors for structural characterization.

Acknowledgements

We are grateful to Dr. H. Pircher for the cDNA clones of the P14 TCR and helpful discussions. We thank Dr. K.M. Müller for the plasmid containing the biotinylation tag and helpful discussions. This work was supported by grants from the EMDO Stiftung and the Schweizerische Nationalfonds.

References

Alam, S.M., Travers, P.J., Wung, J.L., Nasholds, W., Redpath, S., Jameson, S.C., Gascoigne, N.R., 1996. T-cell-receptor affinity and thymocyte positive selection. Nature 381, 616.

Altman, J.D., Moss, P.A.H., Goulder, P.J.R., Barouch, D.H., McHeyzer-Williams, M.G., Bell, J.I., McMichael, A.J., Davis, M.M., 1996. Phenotypic analysis of antigen-specific T lymphocytes. Science 274, 94.

Bachmann, M.F., Sebzda, E., Kündig, T.M., Shahinian, A., Speiser, D.E., Mak, T.W., Ohashi, P.S., 1996. T cell responses are governed by avidity and co-stimulatory thresholds. Eur. J. Immunol. 26, 2017.

Bayer, E.A., Ehrlich-Rogozinski, S., Wilchek, M., 1996. Sodium dodecylsulfate-polyacrylamide gel electrophoretic method for assessing the quaternary state and comparative thermostability of avidin and streptavidin. Electrophoresis 17, 1319.

Brinkmann, U., Mattes, R.E., Buckel, P., 1989. High-level expression of recombinant genes in *Escherichia coli* is dependent on the availability of the dnaY gene product. Gene 85, 109.

Buchner, J., Pastan, I., Brinkmann, U., 1992. A method for increasing the yield of properly folded recombinant fusion proteins: single-chain immunotoxins from renaturation of bacterial inclusion bodies. Anal. Biochem. 205, 263.

Buchner, J., Rudolph, R., 1991. Routes to active proteins from transformed microorganisms. Curr. Opin. Biotechnol. 2, 532.

Chang, H.C., Bao, Z., Yao, Y., Tse, A.G., Goyarts, E.C., Madsen, M., Kawasaki, E., Brauer, P.P., Sacchettini, J.C., Nathenson, S.G., Reinherz, E.L., 1994. A general method for facilitating heterodimeric pairing between two proteins: application to expression of α and β T-cell receptor extracellular segments. Proc. Natl. Acad. Sci. USA 91, 11408.

Chothia, C., Jones, E.Y., 1997. The molecular structure of cell adhesion molecules. Annu. Rev. Biochem. 66, 823.

Chung, S., Wucherpfennig, K.W., Friedman, S.M., Hafler, D.A., Strominger, J.L., 1994. Functional three-domain single-chain T-cell receptors. Proc. Natl. Acad. Sci. USA 91, 12654.

Corr, M., Slanetz, A.E., Boyd, L.F., Jelonek, M.T., Khilko, S., al-Ramadi, B.K., Kim, Y.S., Maher, S.E., Bothwell, A.L., Margulies, D.H., 1994. T cell receptor–MHC class I peptide interactions: affinity, kinetics, and specificity. Science 265, 946.

Crameri, A., Raillard, S.A., Bermudez, E., Stemmer, W.P., 1998. DNA shuffling of a family of genes from diverse species accelerates directed evolution. Nature 391, 288.

Dal Porto, J., Johansen, T.E., Catipovic, B., Parfiit, D.J., Tuveson, D., Gether, U., Kozlowski, S., Fearon, D.T., Schneck, J.P., 1993. A soluble divalent class I major histocompatibility complex molecule inhibits alloreactive T cells at nanomolar concentrations. Proc. Natl. Acad. Sci. USA 90, 6671.

Davis, M.M., Boniface, J.J., Reich, Z., Lyons, D., Hampl, J., Arden, B., Chien, Y., 1998. Ligand recognition by αβ T cell receptors. Annu. Rev. Immunol. 16, 523.

Ding, Y.H., Smith, K.J., Garboczi, D.N., Utz, U., Biddison, W.E., Wiley, D.C., 1998. Two human T cell receptors bind in a similar diagonal mode to the HLA–A2/Tax peptide complex using different TCR amino acids. Immunity 8, 403.

Ding, Y.H., Baker, B.M., Garboczi, D.N., Biddison, W.E., Wiley, D.C., 1999. Four A6-TCR/peptide/HLA-A2 structures that generate very different T cell signals are nearly identical. Immunity 11, 45–56.

Dunbar, P.R., Ogg, G.S., Chen, J., Rust, N., van der Bruggen, P., Cerundolo, V., 1998. Direct isolation, phenotyping and cloning of low-frequency antigen-specific cytotoxic T lymphocytes from peripheral blood. Curr. Biol. 8, 413.

Freund, C., Ross, A., Guth, B., Plückthun, A., Holak, T.A., 1993. Characterization of the linker peptide of the single-chain Fv fragment of an antibody by NMR spectroscopy. FEBS Lett. 320, 97.

Gallimore, A., Dumrese, T., Hengartner, H., Zinkernagel, R.M., Rammensee, H.G., 1998a. Protective immunity does not correlate with the hierarchy of virus-specific cytotoxic T cell responses to naturally processed peptides. J. Exp. Med. 187, 1647.

Gallimore, A., Glithero, A., Godkin, A., Tissot, A.C., Plückthun, A., Elliott, T., Hengartner, H., Zinkernagel, R., 1998b. Induction and exhaustion of lymphocytic choriomeningitis virus-specific cytotoxic T lymphocytes visualized using soluble tetrameric major histocompatibility complex class I-peptide complexes. J. Exp. Med. 187, 1383.

Garboczi, D.N., Ghosh, P., Utz, U., Fan, Q.R., Biddison, W.E.,

Wiley, D.C., 1996a. Structure of the complex between human T-cell receptor, viral peptide and HLA-A2. Nature 384, 134.

Garboczi, D.N., Utz, U., Ghosh, P., Seth, A., Kim, J., VanTienhoven, E.A., Biddison, W.E., Wiley, D.C., 1996b. Assembly, specific binding, and crystallization of a human TCR-αβ with an antigenic Tax peptide from human T lymphotropic virus type 1 and the class I MHC molecule HLA-A2. J. Immunol. 157, 5403.

Garcia, K.C., Degano, M., Pease, L.R., Huang, M., Peterson, P.A., Teyton, L., Wilson, I.A., 1998. Structural basis of plasticity in T cell receptor recognition of a self peptide–MHC antigen. Science 279, 1166.

Garcia, K.C., Degano, M., Stanfield, R.L., Brunmark, A., Jackson, M.R., Peterson, P.A., Teyton, L., Wilson, I.A., 1996. An αβ T cell receptor structure at 2.5 Å and its orientation in the TCR–MHC complex. Science 274, 209.

Ge, L., Knappik, A., Pack, P., Freund, C., Plückthun, A., 1995. Expressing antibodies in *Escherichia coli*. In: Borrebaeck, C.A.K. (Ed.), Antibody Engineering, A Practical Approach, Oxford University Press, Oxford, p. 229.

Gill, S.C., von Hippel, P.H., 1989. Calculation of protein extinction coefficients from amino acid sequence data. Anal. Biochem. 182, 319.

Giver, L., Arnold, F.H., 1998. Combinatorial protein design by in vitro recombination. Curr. Opin. Chem. Biol. 2, 335.

Golden, A., Khandekar, S.S., Osburne, M.S., Kawasaki, E., Reinherz, E.L., Grossman, T.H., 1997. High-level production of a secreted, heterodimeric αβ murine T-cell receptor in *Escherichia* coli. J. Immunol. Methods 206, 163.

Gregoire, C., Malissen, B., Mazza, G., 1996. Characterization of T cell receptor single-chain Fv fragments secreted by myeloma cells. Eur. J. Immunol. 26, 2410.

Hudrisier, D., Mazarguil, H., Laval, F., Oldstone, M.B.A., Gairin, J.E., 1996. Binding of viral antigens to major histocompatibility complex class I H-2D^{b} molecules is controlled by dominant negative elements at peptide non-anchor residues. Implications for peptide selection and presentation. J. Biol. Chem. 271, 17829.

Joao, H.C., Scragg, I.G., Dwek, R.A., 1992. Effects of glycosylation on protein conformation and amide proton exchange rates in RNase B. FEBS Lett. 307, 343.

Jung, S., Plückthun, A., 1997. Improving in vivo folding and stability of a single-chain Fv antibody fragment by loop grafting. Protein Eng. 10, 959.

Kabat, E.A., Wu, T.T., Perry, H.M., Gottesman, K.S., Foeller, C., 1991. In: Sequences of proteins of immunological interest, vol. 1–3, Department of Health and Human Services NIH Pub. 91-3242.

Khandekar, S.S., Bettencourt, B.M., Wyss, D.F., Naylor, J.W., Brauer, P.P., Huestis, K., Dwyer, D.S., Profy, A.T., Osburne, M.S., Banerji, J., Jones, B., 1997. Conformational integrity and ligand binding properties of a single chain T-cell receptor expressed in *Escherichia coli*. J. Biol. Chem. 272, 32190.

Kiefhaber, T., Rudolph, R., Kohler, H.H., Buchner, J., 1991. Protein aggregation in vitro and in vivo: a quantitative model of the kinetic competition between folding and aggregation. Biotechnology (NY) 9, 825.

Klemm, J.D., Schreiber, S.L., Crabtree, G.R., 1998. Dimerization as a regulatory mechanism in signal transduction. Annu. Rev. Immunol. 16, 569.

Knappik, A., Plückthun, A., 1995. Engineered turns of a recombinant antibody improve its in vivo folding. Protein Eng. 8, 81.

Kubo, R.T., Born, W., Kappler, J.W., Marrack, P., Pigeon, M., 1989. Characterization of a monoclonal antibody which detects all murine αβ T cell receptors. J. Immunol. 142, 2736.

Kurucz, I., Titus, J.A., Jost, C.R., Segal, D.M., 1995. Correct disulfide pairing and efficient refolding of detergent-solubilized single-chain Fv proteins from bacterial inclusion bodies. Mol. Immunol. 32, 1443.

Lin, A.Y., Devaux, B., Green, A., Sagerstrom, C., Elliott, J.F., Davis, M.M., 1990. Expression of T cell antigen receptor heterodimers in a lipid-linked form. Science 249, 677.

Lyons, D.S., Lieberman, S.A., Hampl, J., Boniface, J.J., Chien, Y., Berg, L.J., Davis, M.M., 1996. A TCR binds to antagonist ligands with lower affinities and faster dissociation rates than to agonists. Immunity 5, 53.

Maeda, Y., Ueda, T., Imoto, T., 1996. Effective renaturation of denatured and reduced immunoglobulin G in vitro without assistance of chaperone. Protein Eng. 9, 95.

Matsui, K., Boniface, J.J., Steffner, P., Reay, P.A., Davis, M.M., 1994. Kinetics of T-cell receptor binding to peptide/I-E^{k} complexes: correlation of the dissociation rate with T-cell responsiveness. Proc. Natl. Acad. Sci. USA 91, 12862.

McMichael, A.J., O'Callaghan, C.A., 1998. A new look at T cells. J. Exp. Med. 187, 1367.

Müller, K.M., Arndt, K.M., Strittmatter, W., Plückthun, A., 1998. The first constant domain (C_H1 and C_L) of an antibody used as heterodimerization domain for bispecific miniantibodies. FEBS Lett. 422, 259.

Murali-Krishna, K., Altman, J.D., Suresh, M., Sourdive, D.J., Zajac, A.J., Miller, J.D., Slansky, J., Ahmed, R., 1998. Counting antigen-specific CD8 T cells: a reevaluation of bystander activation during viral infection. Immunity 8, 177.

Ohashi, P.S., Zinkernagel, R.M., Leuscher, I., Hengartner, H., Pircher, H., 1993. Enhanced positive selection of a transgenic TCR by a restriction element that does not permit negative selection. Int. Immunol. 5, 131.

Oxenius, A., Bachmann, M.F., 1997. Similar ligand densities required for restimulation and effector function of cytotoxic T cells. Cell. Immunol. 179, 16.

Pack, P., Plückthun, A., 1992. Miniantibodies: use of amphipathic helices to produce functional, flexibly linked dimeric F_v fragments with high avidity in *Escherichia coli*. Biochemistry 31, 1579.

Patten, P.A., Howard, R.J., Stemmer, W.P., 1997. Applications of DNA shuffling to pharmaceuticals and vaccines. Curr. Opin. Biotechnol. 8, 724.

Pecorari, F., Tissot, A.C., Plückthun, A., 1999. Folding, heterodimeric association and specific peptide recognition of a murine αβ T-cell receptor expressed in *Escherichia coli*. J. Mol. Biol. 285, 1831.

Pircher, H., Michalopoulos, E.E., Iwamoto, A., Ohashi, P.S., Baenziger, J., Hengartner, H., Zinkernagel, R.M., Mak, T.W., 1987. Molecular analysis of the antigen receptor of virus-specific cytotoxic T cells and identification of a new V alpha family. Eur. J. Immunol. 17, 1843.

Pircher, H., Rebai, N., Groettrup, M., Gregoire, C., Speiser, D.E., Happ, M.P., Palmer, E., Zinkernagel, R.M., Hengartner, H., Malissen, B., 1992. Preferential positive selection of $V\alpha_2^+$ $CD8^+$ T-cells in mouse strains expressing both $H\text{-}2^k$ and T-cell receptor Vα a haplotypes: determination with a $V\alpha_2$-specific monoclonal antibody. Eur. J. Immunol. 22, 399.

Pircher, H., Brduscha, K., Steinhoff, U., Kasai, M., Mizuochi, T., Zinkernagel, R.M., Hengartner, H., Kyewski, B., Müller, K.P., 1993. Tolerance induction by clonal deletion of CD4+8+ thymocytes in vitro does not require dedicated antigen-presenting cells. Eur. J. Immunol. 23, 669.

Plaksin, D., Polakova, K., McPhie, P., Margulies, D.H., 1997. A three-domain T cell receptor is biologically active and specifically stains cell surface MHC/peptide complexes. J. Immunol. 158, 2218.

Plückthun, A., Pack, P., 1997. New protein engineering approaches to multivalent and bispecific antibody fragments. Immunotechnology 3, 83.

Powell, L.M., Pain, R.H., 1992. Effects of glycosylation on the folding and stability of human, recombinant and cleaved alpha 1-antitrypsin. J. Mol. Biol. 224, 241.

Proba, K., Wörn, A., Honegger, A., Plückthun, A., 1998. Antibody scFv fragments without disulfide bonds made by molecular evolution. J. Mol. Biol. 275, 245.

Rozema, D., Gellman, S.H., 1996. Artificial chaperone-assisted refolding of carbonic anhydrase B. J. Biol. Chem. 271, 3478.

Rudolph, R., Lilie, H., 1996. In vitro folding of inclusion body proteins. FASEB J. 10, 49.

Schatz, P.J., 1993. Use of peptide libraries to map the substrate specificity of a peptide-modifying enzyme: a 13 residue consensus peptide specifies biotinylation in *Escherichia coli*. Biotechnology (NY) 11, 1138.

Schodin, B.A., Schlueter, C.J., Kranz, D.M., 1996. Binding properties and solubility of single-chain T cell receptors expressed in *E. coli*. Mol. Immunol. 33, 819.

Schoel, B., Zügel, U., Ruppert, T., Kaufmann, S.H., 1994. Elongated peptides, not the predicted nonapeptide stimulate a major histocompatibility complex class I-restricted cytotoxic T lymphocyte clone with specificity for a bacterial heat shock protein. Eur. J. Immunol. 24, 3161.

Scott, C.A., Garcia, K.C., Carbone, F.R., Wilson, I.A., Teyton, L., 1996. Role of chain pairing for the production of functional soluble IA major histocompatibility complex class II molecules. J. Exp. Med. 183, 2087.

Stempfer, G., Höll-Neugebauer, B., Kopetzki, E., Rudolph, R., 1996. A fusion protein designed for noncovalent immobilization: stability, enzymatic activity, and use in an enzyme reactor. Nature Biotechnol. 14, 481.

Studier, F.W., Rosenberg, A.H., Dunn, J.J., Dubendorff, J.W., 1990. Use of T7 RNA polymerase to direct expression of cloned genes. Methods. Enzymol. 185, 60.

Sykulev, Y., Brunmark, A., Jackson, M., Cohen, R.J., Peterson, P.A., Eisen, H.N., 1994. Kinetics and affinity of reactions between an antigen-specific T cell receptor and peptide–MHC complexes. Immunity 1, 15.

Sykulev, Y., Cohen, R.J., Eisen, H.N., 1995. The law of mass action governs antigen-stimulated cytolytic activity of CD8+ cytotoxic T lymphocytes. Proc. Natl. Acad. Sci. USA 92, 11990.

Tams, J.W., Welinder, K.G., 1998. Glycosylation and thermodynamic versus kinetic stability of horseradish peroxidase. FEBS Lett. 421, 234.

Townsend, A.R., Rothbard, J., Gotch, F.M., Bahadur, G., Wraith, D., McMichael, A.J., 1986. The epitopes of influenza nucleoprotein recognized by cytotoxic T lymphocytes can be defined with short synthetic peptides. Cell 44, 959.

Traunecker, A., Dolder, B., Oliveri, F., Karjalainen, K., 1989. Solubilizing the T-cell receptor—problems in solution. Immunol. Today 10, 29.

Tsumoto, K., Shinoki, K., Kondo, H., Uchikawa, M., Juji, T., Kumagai, I., 1998. Highly efficient recovery of functional single-chain Fv fragments from inclusion bodies overexpressed in *Escherichia coli* by controlled introduction of oxidizing reagent—application to a human single-chain Fv fragment. J. Immunol. Methods 219, 119.

van der Merwe, P.A., Barclay, A.N., 1994. Transient intercellular adhesion: the importance of weak protein–protein interactions. Trends Biochem. Sci. 19, 354.

Wang, C., Eufemi, M., Turano, C., Giartosio, A., 1996. Influence of the carbohydrate moiety on the stability of glycoproteins. Biochemistry 35, 7299.

Wang, J., Lim, K., Smolyar, A., Teng, M., Liu, J., Tse, A.G., Hussey, R.E., Chishti, Y., Thomson, C.T., Sweet, R.M., Nathenson, S.G., Chang, H.C., Sacchettini, J.C., Reinherz, E.L., 1998. Atomic structure of an αβ T cell receptor (TCR) heterodimer in complex with an anti-TCR fab fragment derived from a mitogenic antibody. EMBO J. 17, 10.

Weber, S., Traunecker, A., Oliveri, F., Gerhard, W., Karjalainen, K., 1992. Specific low-affinity recognition of major histocompatibility complex plus peptide by soluble T-cell receptor. Nature 356, 793.

Willcox, B.E., Gao, G.F., Wyer, J.R., Ladbury, J.E., Bell, J.I., Jakobsen, B.K., van der Merwe, P.A., 1999. TCR binding to peptide–MHC stabilizes a flexible recognition interface. Immunity 10, 357–365.

Withka, J.M., Wyss, D.F., Wagner, G., Arulanandam, A.R., Reinherz, E.L., Recny, M.A., 1993. Structure of the glycosylated adhesion domain of human T lymphocyte glycoprotein CD2. Structure 1, 69.

Wülfing, C., Plückthun, A., 1994. Correctly folded T-cell receptor fragments in the periplasm of *Escherichia coli*. Influence of folding catalysts. J. Mol. Biol. 242, 655.

Wülfing, C., Plückthun, A., 1995. T-cell receptor signal sequences. Immunol. Today 16, 405.

Wung, J.L., Gascoigne, N.R., 1996. Antibody screening for secreted proteins expressed in *Pichia pastoris*. Biotechniques 21, 808.

Young, A.C., Zhang, W., Sacchettini, J.C., Nathenson, S.G., 1994. The three-dimensional structure of $H\text{-}2D^b$ at 2.4 Å resolution: implications for antigen-determinant selection. Cell 76, 39.